tadata, citation and similar papers at core.ac.uk

SCIENCE DIRECT®

Precambrian Research

ELSEVIER

Precambrian Research 138 (2005) 208–224

www.elsevier.com/locate/precamres

Combined micro-Fourier transform infrared (FTIR) spectroscopy and micro-Raman spectroscopy of Proterozoic acritarchs: A new approach to Palaeobiology

Craig P. Marshall [a,*], Emmanuelle J. Javaux [b], Andrew H. Knoll [c], Malcolm R. Walter [a]

[a] *Australian Centre for Astrobiology, Macquarie University, Sydney, NSW 2109, Australia*
[b] *Department of Astrophysics, Geophysics and Oceanography, University of Liège, 17 Allée du 6 Août, B5c, 4000 Liège (Sart-Tilman), Belgium*
[c] *Department of Organismic and Evolutionary Biology, Harvard University, 26 Oxford Street, Cambridge, MA 02138, USA*

Received 11 February 2005; received in revised form 6 May 2005; accepted 13 May 2005

Abstract

Micro-scale analytical techniques permit correlation of chemistry with morphology of individual Proterozoic acritarchs (organic-walled microfossils), and thus provide new approaches for elucidating their biological affinities. A combination of micro-Fourier transform infrared (FTIR) spectroscopy and laser micro-Raman spectroscopy was used to investigate the organic structure and composition of individual acritarchs. Well preserved Neoproterozoic acritarchs from the Tanana Formation, Australia (ca. 590–565 Ma), and Mesoproterozoic acritarchs from the Roper Group (1.5–1.4 Ga), Australia, and Ruyang Group, China (1.4–1.3 Ga, age poorly resolved but certainly >1000 Ma and <1625 Ma) have thermal maturities that range from immature to oil window. FTIR spectra of *Tanarium conoideum* from the Tanana Formation contain intense aliphatic C–H stretching bands in the 2900 cm^{-1} region relative to the C=C aromatic ring stretching band at 1600 cm^{-1}. This FTIR spectrum is consistent with the FTIR spectra obtained from algaenans isolated from extant chlorophyte and eustigmatophyte microalgae. FTIR spectra of *Leiosphaeridia* sp. from the Tanana Formation contain a less intense aliphatic C–H stretching band relative to the C=C aromatic ring stretching band. By comparison, the spectra acquired from the Mesoproterozoic acritarchs were dominated by C=C aromatic ring stretching bands at 1600 cm^{-1} relative to moderate-weak CH_3 terminal groups (1345 cm^{-1}), C–H aliphatic stretching (3000–2700 cm^{-1}), and C=O (1710 cm^{-1}), although some differences in biopolymer composition occurred between species. Curve-fitting of the aliphatic C–H_x stretching region provides greater insight into the aliphatic structures of the acritarchs. The CH_2/CH_3 intensity ratio can be used to assess the relative chain length and degree of branching. Organic material in the *Tanarium conoideum* consists of straight long chain hydrocarbons, while the other acritarchs contain hydrocarbons consisting of short chains that are highly branched. In this study it was found that Raman spectroscopy does not provide additional information

* Corresponding author at: Vibrational Spectroscopy Facility, School of Chemistry, The University of Sydney, NSW 2006, Australia. Tel.: +61 2 9351 3994; fax: +61 2 9351 3329.
E-mail address: c.marshall@chem.usyd.edu.au (C.P. Marshall).

0301-9268/$ – see front matter © 2005 Elsevier B.V. All rights reserved.
doi:10.1016/j.precamres.2005.05.006

about biopolymer composition of Proterozoic acritarchs, but rather offers complementary data regarding the aromaticity and degree of saturation of the macromolecular structure of acritarch cysts.
© 2005 Elsevier B.V. All rights reserved.

Keywords: Fourier transform infrared (FTIR) spectroscopy; Raman spectroscopy; Acritarchs; Biopolymers

1. Introduction

Acritarchs are organic-walled, acid-resistant microfossils of unknown biological affinities, ranging in age from the Proterozoic through to nearly the present. Conventionally, acritarchs have been interpreted as the cysts of eukaryotic algae, but the group probably also includes prokaryotic sheaths, heterotroph protists, vegetative parts of cells or multicellular organisms (Butterfield, 2004), and even animal egg cases (Van Waveren, 1992).

During the last three decades several attempts have been made to establish links between acritarchs and modern phytoplankton taxa (Wall, 1962; Downie et al., 1963; Staplin et al., 1965; Tappan, 1980; Martin, 1993; Sarjeant and Stancliffe, 1994; Colbath and Grenfell, 1995). Colbath and Grenfell (1995), for example, suggested that only the Prasinophyceae, a division of green algae, had a record extending back to the Proterozoic, with other algal groups appearing in the Silurian or later. However, fossil evidence and molecular clock analyses (Su et al., 2004) both indicate a much earlier origin of photosynthetic eukaryotes, suggesting broader candidate affinities for Proterozoic acritarchs. Eukaryotic diversification began no later than the late Paleoproterozoic and by the end of the Mesoproterozoic multiple crown group phyla must have existed (Douzery et al., 2004; Knoll, 1996; Anbar and Knoll, 2002), as shown by the presence of multicellular red algae in ∼1.2 Ga chert from Arctic Canada (Butterfield, 2000). More recently, in palynological studies of Neoproterozoic acritarchs from the Australian Centralian Superbasin (Grey, 1998; Arouri et al., 1999, 2000), affinity to green algae (including prasinophytes) has been shown for a few acritarch species. Ultrastructural studies (Talyzina and Moczydlowska, 2000) on Lower Cambrian acritarchs also revealed an affinity to Chlorococcalean green algae for a leiosphere and a prasinophyte affinity for *Tasmanites* sp.

Until recently, evidence for morphological and taxonomic diversification of acritarchs has been restricted to the Neoproterozoic (600 Ma). However, recent morphological studies of acritarchs from the Mesoproterozoic (1.5–1.4 Ga) Roper Group in northern Australia suggest an earlier diversification than previously known (Javaux et al., 2001). Morphological and ultrastructural details of these well preserved acritarchs differentiate them from prokaryotic microfossils and reveal a moderate degree of both protistan diversity and cellular complexity (Javaux et al., 2001, 2003, 2004a,b). However, the biological affinities of these microfossils have not been determined below the level of domain.

Palaeontologists have long wished to link diagnostic organic molecules directly to individual microfossil taxa, in part because this might establish the systematic relationships of otherwise problematic fossils. Isolating pure monospecific assemblages is difficult and time-consuming, but a new approach, described here, consists of applying micro-scale analytical techniques to very small samples, including individual microfossils. Specifically, we have developed methods to apply micro-Fourier transform infrared (FTIR) spectroscopy and micro-laser Raman spectroscopy to individual acritarchs.

1.1. Previous studies on Organic Geochemistry of Acritarchs

A number of studies have investigated sporopollenin occurrence in spores and pollen (for example, Brooks and Shaw, 1971), but few have focused on resistant biopolymers in fossil algae. Acritarchs are composed of organic material that is mechanically resistant; however, its chemical composition is poorly known, being chemically inert, except to oxidation and carbonization. Kjellstrom (1968) estimated by interpretation of micro-FTIR spectra, that certain particularly ubiquitous acritarchs (*Leiosphaeridia* spp.) probably contained saturated fatty acid derivatives similar to those from spores and pollen grains. Moldowan and Talyzina (1998) and Talyzina et al. (2000) detected

dinoflagellate specific biomarkers, dinosteranes and 4α-methyl-24-ethylsteranes, in the pyrolysates of Early Cambrian mixed acritarch concentrates. However, even these careful analyses tell us only that biomarker-producing dinoflagellates and cyst-producing cells lived in the same environment. We know of no reports these biomarkers from older, individually analysed acritarchs.

Arouri et al. (1999) analysed two Neoproterozoic acritarchs, *Multifronsphaeridium pelorium* and the informally designated Species A, by Scanning Electron Microscopy (SEM), Transmission Electron Microscopy (TEM), micro-FTIR spectroscopy, py-GC/MS, and thermal desorption MS. The macromolecular structure of *Multifronsphaeridium pelorium* and Species A consisted of short *n*-alkylpolymethylenic chains, probably linked via ether/ester bonds, with possibly a small aromatic content. They concluded that the ultrastructural and molecular results show evidence for a phylogenetic relationship between these acritarchs and Chlorophyceae (see Versteegh and Blokker, 2004, for commentary). In a further study, Arouri et al. (2000) analysed a range of Neoproterozoic acritarchs (*Tanarium* sp., *Hocosphaeridium scaberfacium*, *Alicesphaeridium medusoidum*, *Chuaria circularis*, *Leiosphaeridia* sp., and *Tasmanites* sp.) by micro-FTIR spectroscopy, py-GC/MS, and laser Raman spectroscopy. They concluded that little chemical data was obtained by micro-FTIR spectroscopy and py-GC/MS and this was consistent with a polyaromatic biomacromolecule of high recalcitrance. In addition, they interpreted their Raman spectra to show a signal attributable to significant carbon ordering characteristic of polyaromatic structures. However, the correct interpretation of their Raman spectra is that the macromolecular network consists of low thermally matured disordered sp^2 carbon. These results led the authors to the conclusion that the acritarchs are composed of a polyaromatic biopolymer indicating a genetic relationship with dinoflagellates. Such studies form a basis for our microchemical analyses of the older acritarchs that provide our earliest well characterized evidence for eukaryotic diversification.

The aims of this paper are to develop a micro-FTIR spectroscopic method tailored to micro-scale characterization of Proterozoic acritarchs, to elucidate their cyst wall biopolymer composition, and, thus, to establish their biological affinities. In this study, we also assess the possibility of using laser Raman spectroscopy to obtain useful information pertaining to biopolymer composition of microfossils. By comparison with biomarker analyses, micro-FTIR and micro-Raman techniques have the great advantages of being applicable on a very small sample (such as one microfossil), of providing data on the chemical composition of microfossils with previously described morphology and ultrastructure, and of avoiding contamination problems. Thus, the techniques used in this study extend the approach of Arouri et al. (1999, 2000) in relating fossil morphology directly to chemical composition.

2. Experimental

2.1. Samples

Acritarch microfossils were isolated from three drill cores (Urapunga 5, 6; Amoco 82/3) in the Roper Group, Australia (1.5–1.4 Ga), two outcrop sections in the Ruyang Group, China (∼1.4–1.3 Ga, age bracketed by radiometric dates of 1625 and 1000 Ma; C-isotopic profile suggests an age greater than 1250 Ma; Xiao et al., 1997), and one drill core (Observatory Hill #1) in the Tanana Formation, Australia (ca. 590–565 Ma). The palaeoecological distribution, morphology and wall ultrastructure of the acritarchs used in this study have been described for Roper and Ruyang samples by Javaux et al. (2001, 2003, 2004a,b) and for the Tanana specimens by Arouri et al. (1999, 2000) and Grey (1998).

2.2. Sample preparation

The drill core was demineralised with HF/HCl acid treatment followed by settling and decantation to extract the acid insoluble acritarch. Single acritarchs were handpicked from kerogen isolate under a steromicroscope using a micropipette. The acritarchs were soaked in dichloromethane for 30 min to remove extraneous surface contaminants. Acritarchs isolated from the Ruyang Group include *Shuiyousphaeridium macroreticulatum*. Acritarchs isolated from the Roper Group include *Satka squamifera*, *Leiosphaeridia tenuissima*, *Leiosphaeridia jacutica*, and *Leiosphaeridia crassa* (Fig. 1). Acritarchs isolated from the Tanana Formation include *Tanarium*

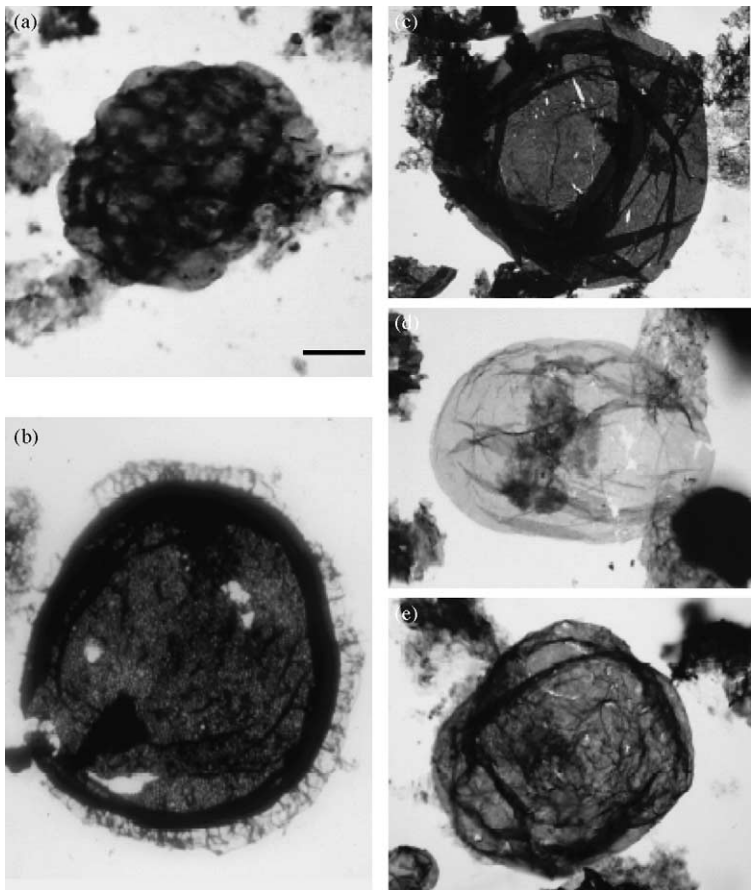

Fig. 1. Light photographs of analyzed species. (a) and (c)–(e): microfossils from the Roper Group, Australia; (b): microfossil from the Ruyang Group, China. (a) *Satka squamifera*; (b) *Shuiyousphaeridium macroreticulatum*; (c) *Leiosphaeridia jacutica*; (d) *Leiosphaeridia tenuissima*; (e) *Leiosphaeridia crassa*. Scale bar in (a) is 15 μm for (a) and (d); 46 μm for (b); 20 μm for (c); 10 μm for (e).

conoideum and *Leiosphaeridia* sp. (Fig. 2b, Arouri et al., 2000, p. 80).

2.3. Microscopy and TAI assessment

Thermal Alteration Index (TAI) observations were made using an Olympus BH2 microscope. The TAI scale of Batten (1996) was used as the standard.

2.4. Micro-Fourier transform infrared (FTIR) spectroscopy

Micro-analytical techniques have been applied to two or three specimens of each taxon. Micro-FTIR spectroscopic analyses were performed using a Bruker IFS66 Fourier transform infrared spectrometer coupled to a Bruker microscope accessory housing a dedicated liquid nitrogen cooled (77 K), narrow-band mercury cadmium telluride detector. The microscope was fitted with an IR/visible Cassegrainian 15× objective (numerical aperture = 0.4). Acritarch samples were placed on potassium bromide slides. Interferograms were acquired in the transmission mode within the range 4000–900 cm^{-1} by accumulating 256 scans at a spectral resolution of 4 cm^{-1}. Spectral bands were assigned with reference to the literature (for example, Painter et al., 1985; Solomon and Carangelo, 1987).

The aliphatic C–H_x stretching zone (3000–2700 cm^{-1}) was studied by curve-fitting analysis using a commercially available data-processing pro-

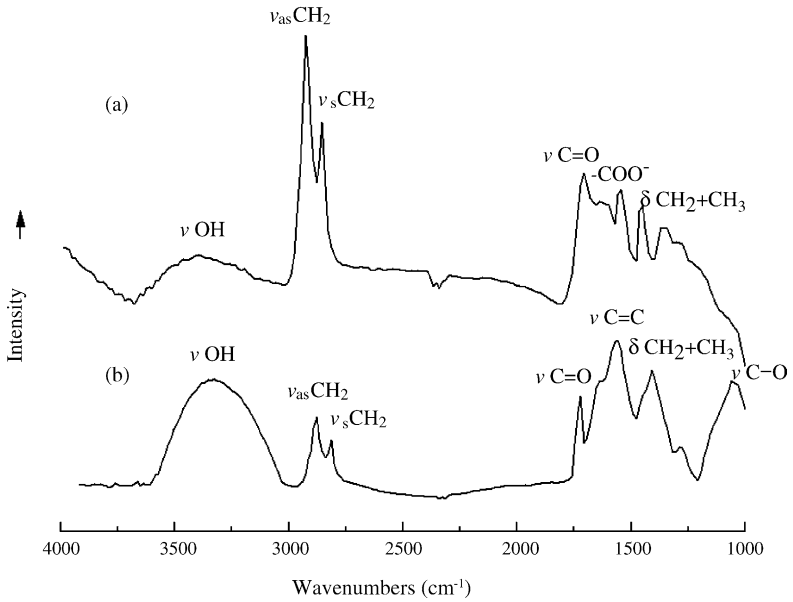

Fig. 2. Representative micro-FTIR spectra of Neoproterozoic acritarchs: (a) *Tanarium 'conoideum* and (b) *Leiosphaeridia* sp. Refer to Table 2 for band assignments.

gram (GRAM/32 software). The aliphatic region was baseline-linearized using an interactive procedure of the program by connecting the left and right points of the interval with a straight line. Positions and number of bands were established from the second derivative of the spectrum. A mix Gaussian/Lorentzian function was used for peak shapes. The parameters were fitted to the experimental envelope by a least squares iterative procedure. In order to determine goodness of fit criteria, the following aspects were considered: standard errors of parameters (chi-squared), local poor fits (indicative of an incorrect choice of the number of component peaks or errors in their half-widths) and the degree of coincidence of the second derivative (original and fitted spectrum). In this work, the parameters investigated were the following:

$$\frac{CH_2}{CH_3} : \frac{\text{intensity } 2920\,\text{cm}^{-1}\text{ band}}{\text{intensity } 2955\,\text{cm}^{-1}\text{ band}} \quad (1)$$

$$\frac{H_{al}}{C_{ar}} : \frac{\text{intensity } 3000\text{–}2700\,\text{cm}^{-1}\text{ region}}{\text{intensity } 1600\,\text{cm}^{-1}\text{ band}} \quad (2)$$

$$\frac{CO}{C_{ar}} : \frac{\text{intensity } 1710\,\text{cm}^{-1}\text{ band}}{\text{intensity } 1600\,\text{cm}^{-1}\text{ band}} \quad (3)$$

The methylene to methyl ratio was determined from the integrated absorbance from the curve-fitted bands at 2920 and 2955 cm^{-1}. This ratio (1) can be considered an estimate of the length of aliphatic chains and a branching index (Lin and Ritz, 1993). The ratio of aliphatic hydrogen content to aromatic carbon (H_{al}/C_{ar}; 2) provides a measure of aromaticity—that is, the proportional abundance of aromatic carbon. The ratio of the carbonyl CO groups to the aromatic carbon content of the acritarchs is given by (CO/C_{ar}; 3).

2.5. Laser micro-Raman spectroscopy

Raman spectra were acquired on a Renishaw Raman Microprobe Laser Raman Spectrometer using a charge coupled detector. The collection optics are based on a Leica DMLM microscope. A refractive glass 50× objective lens was used to focus the laser onto a 2 μm spot to collect the backscattered radiation. The 514.5 nm line of a 5 W Ar^+ laser (Spectra-Physics Stabilite 2017 laser) orientated normal to the sample was used to excite the sample. Surface laser powers of 1.0–1.5 mW were used to minimize laser induced heating of the acritarchs. An accumulation time of 30 s and 10 scans were used which gave adequate

signal-to-noise ratio of the spectra. The scan ranges were 1000–1800 cm^{-1} in the carbon first-order region. Acritarchs were deposited on clean aluminum microscope slides and irradiated with the laser to obtain spectra.

3. Results

3.1. TAI assessments

Table 1 lists the acritarch genera studied here, along with drill hole information, stratigraphic location, and TAI, as determined from the scale of Batten (1996). Most palynomorphs, including acritarchs, show sequential colour and structural changes in response to increasing depth of burial related to the thermal history of the enclosing sediment. The acritarchs used in this study show sequential colour changes from yellow to orange–brown (Table 1) corresponding to a TAI range from 1/2 to 4, approximately equivalent to a vitrinite reflectance of 0.2–0.75% (Senftle and Landis, 1991; Traverse, 1988). These thermal maturity indicators show that the organic matter in the acritarchs ranges from immature to oil window (mature). The low thermal maturity of these acritarchs makes them ideally suited for microchemical analysis. Nevertheless, while morphologically well preserved, these acritarchs have undergone some degree of diagenesis, potentially removing more labile components and leaving the more robust and selectively preserved macromolecular structures. Therefore, it is relevant to compare these selectively preserved biopolymers with non-hydrolizable biomacromolecules isolated from extant microorganisms.

Several criteria have been proposed to differentiate eukaryotic from prokaryotic fossil cells (Javaux et al., 2003 and references therein). Previous TEM and SEM studies (Javaux et al., 2001, 2003, 2004a,b) indicate that some Mesoproterozoic acritarchs display complex surface ornaments, wall structures and/or multi-layered wall ultrastructures unknown in prokaryotic cells but similar in general to those of extant protists. The chemical composition of the acritarch cyst might also reveal eukaryotic attributes, but in addition, biopolymer composition may elucidate the finer-scale systematic affinities of microfossils, when morphology and ultrastructure are inadequate for the task.

3.2. General IR Characteristics of the Acritarchs

Typical peak assignments and intensities observed by micro-FTIR spectroscopy for each acritarch sample are given in Table 2.

The one acritarch that contains abundant aliphatic structures, as indicated by the very strong aliphatic C–H_x bands (strong methylene stretching and bending band at 2930–2860 and 1450 cm^{-1}, respectively) is *Tanarium conoideum* from the Neoproterozoic Tanana Formation (Fig. 2a). The spectrum shows absorptions

Table 1
Acritarch genera studied here, along with their drill hole information, stratigraphic location, and TAI as determined from the scale of Batten (1996)

Acritarch	Stratigraphy	Drill hole	Acritarch colour	TAI	Degree of maturation	Equilivant R_0
Shuiyousphaeridium macroreticulatum	Ruyang Group	SYG 6 section	Orange–brown to brown	3–4	Early to mid mature	0.5–0.75
Satka squamifera	Roper Group	A 82/3 161.7 m	Orange–brown	3–4	Mid mature	0.6
Leiosphaeridia tenuissima	Roper Group	U6 230.8 m	Yellow–light brown	2–3	Immature to early mature	0.3–0.5
Leiosphaeridia jacutica	Roper Group	U6 230.8 m	Yellow–light brown	2–3	Immature to early mature	0.3–0.5
Leiosphaeridia crassa	Roper Group	U6 230.8 m	Yellow–light brown	2–3	Immature to early mature	0.3–0.5
Tanarium conoideum	Tanana Formation	Observatory Hill #1 233.0 m	Yellow	1/2–2	Immature	0.2–0.3
Leiosphaeridia sp.	Tanana Formation	Observatory Hill #1 233.0 m	Yellow	1/2–2	Immature	0.2–0.3

Table 2
Typical peak assignments and intensities observed by micro-FTIR spectroscopy for each acritarch sample

Wavenumber (cm^{-1})	Assignment	*Tanarium conoideum*	*Leiosphaeridia* sp.	*Leiosphaeridia tenuissima*	*Leiosphaeridia jacutica*	*Leiosphaeridia crassa*	*Shuiyousphaeridium macroreticulatum*	*Satka squamifera*
3350–3450	O─H stretch	W	S	M	M	M	M	M
2920	Antisymmetric methylene CH_2 stretch	S	M	W	W	W	W	W
2850	Symmetric methylene CH_2 stretch	S	M	W	W	W	W	W
1710	Carbonyl C═O stretch	W	S	Shoulder	Shoulder	Shoulder	W	W
1600	C═C aromatic ring stretch	Np	S	S	S	S	S	S
1532	Aliphatic COOH	Np	Np	Shoulder	Shoulder	Shoulder	Shoulder	S
1450	Methylene CH_2 bend	S	S	Np	Np	Np	Np	W
1345	Terminal methyl CH_3	Np	Np	S	S	S	S	S
1275	C─O stretching aliphatic ethers	Np	S	W	W	W	W	W
900–700	═C─H aromatic deformation	Np	Np	W	W	W	W	W

W, weak; M, moderate; S, strong; and Np, not present.

centered at: a low broad absorption at 3468 cm^{-1} assigned to alcoholic OH, phenolic OH, and/or carboxylic OH; strong narrow aliphatic absorptions centered at 2920 and 2850 cm^{-1} assigned to asymmetric stretching vibrations from CH_2 and symmetric stretching vibrations from CH_2 methylene groups, respectively; a weak absorption centered at 1710 cm^{-1} assigned to the vibration of carbonyl C=O; moderate absorptions of deformation bending of CH_2 and CH_3 centered at 1450 cm^{-1}; and minor absorptions of ether (C–O) bonding between 1200 and 1000 cm^{-1}. A strong methylene stretching and bending band (2930–2860 and 1450 cm^{-1}, respectively) and a weak methyl band indicate a long-chain linear aliphatic structure. The observation of abundant aliphatic structures of cell wall organic material for this acritarch is consistent with that of algaenans isolated from green microalgae (for example, Gelin et al., 1999 and references therein). This representative spectrum acquired from *Tanarium conoideum* is in disagreement with that spectrum obtained from the *Tanarium conoideum* acritarch in Fig. 4 of Arouri et al. (2000). The spectrum in Fig. 4 of Arouri et al. (2000) shows little to no vibration of organic material, and in addition the spectra are heavily dominated by water and carbon dioxide, suggesting instrument or sample preparation problems.

The FTIR spectrum obtained from analyses of *Leiosphaeridia* sp., differs substantially from that of *Tanarium conoideum*. Spectra obtained from *Tanarium conoideum* show a greater aliphatic character than the *Leiosphaeridia* sp. even though these microfossils are isolated from the same core interval. This clearly shows that the inferred differences in biopolymer composition are controlled by the biological source rather than thermal maturity. A representative micro-FTIR spectrum obtained from a single *Leiosphaeridia* sp. acritarch from the Tanana Formation is shown in Fig. 2b. The spectrum shows absorptions centered at: a strong broad absorption at 3468 cm^{-1} assigned to alcoholic OH, phenolic OH, and/or carboxylic OH; strong narrow aliphatic absorptions centered at 2920 and 2850 cm^{-1} assigned to asymmetric stretching vibrations from CH_2 and symmetric stretching vibrations from CH_2 methylene groups, respectively; a moderate absorption centered at 1710 cm^{-1} assigned to the vibration of carbonyl C=O; a strong absorption of olefinic C=C centered at 1600 cm^{-1}; moderate absorptions of deformation bending of CH_2 and CH_3 centered at 1450 cm^{-1}; and a strong broad absorption of aliphatic ether (C–O) bonding centered at 1090 cm^{-1}. Closer inspection of the line-shape and relative magnitude of the aliphatic C–H_x stretching region, 3000–2700 cm^{-1}, shows a slight shoulder at 2960 cm^{-1} (asy C–H str of methyl groups) and a low width of the band centered at 2920 cm^{-1}, which indicates a substantial contribution of polymethylenic chains with a low degree of branching.

Representative micro-FTIR spectra acquired for three leiospheres in the Mesoproterozoic Roper assemblage (*Leiosphaeridia crassa*, *L. jacutica*, *L. tenuissima*), are similar and for brevity the spectra acquired from *L. jacutica* and *Satka squamifera* are shown in Fig. 3a and b, respectively. The spectra show absorptions centered at: a strong broad absorption at

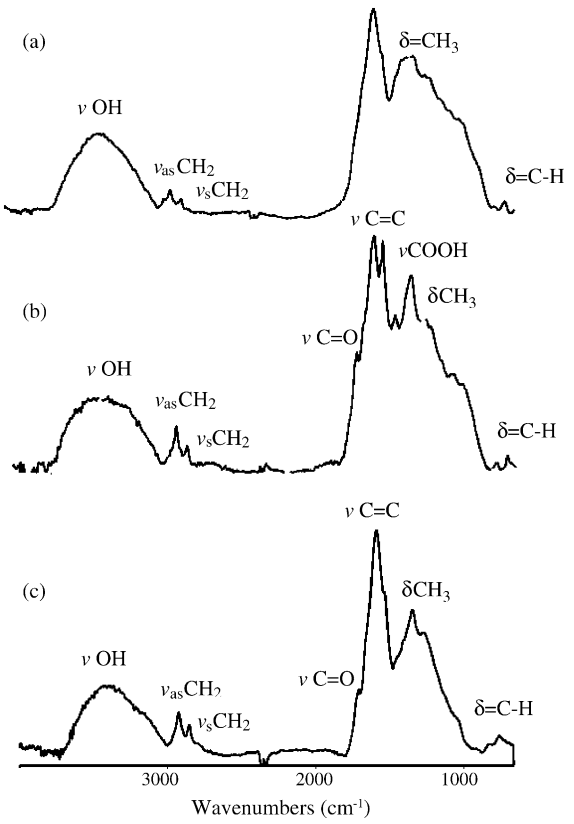

Fig. 3. Representative micro-FTIR spectra of Mesoproterozoic acritarchs: (a) *Leiosphaeridia jacutica*; (b) *Satka squamifera*; and (c) *Shuiyousphaeridium macroreticulatum*. Refer to Table 2 for band assignments.

3379 cm^{-1} assigned to alcoholic OH, phenolic OH, and/or carboxylic OH; medium aliphatic absorptions centered at 2920 and 2850 cm^{-1} assigned to asymmetric stretching vibrations from CH_2 and symmetric stretching vibrations from CH_2 methylene groups, respectively; a slight absorption centered at 1710 cm^{-1} assigned to the vibration of carbonyl C=O for the spectrum acquired from *Satka squamifera*; a strong absorption of aromatic C=C centered at 1600 cm^{-1}; a weak absorption of aliphatic carboxyl COOH at 1532 cm^{-1} for the spectrum acquired from *Satka squamifera*; a moderate absorption of deformation bending of terminal methyl CH_3 groups centered at 1345 cm^{-1}; and a weak absorption centered at 760 cm^{-1} assigned to =C–H aromatic out-of-plane vibration. A slight shoulder appears at 2960 cm^{-1} (asy C–H str of methyl groups) for both spectra; however, this shoulder is more pronounced in the spectrum acquired from *L. jacutica*, which indicates a substantial contribution of branched polymethylenic chains. Notable differences between the *Leiosphaeridia* and *Satka squamifera* spectra include the higher contribution of aliphatic functionality and carbon–oxygen functional groups in the latter. The aromatic nature of these acritarchs could reflect biology or thermal maturity (oil window compared to immature from the Tanana Formation). However, it is interesting to note that the *Satka squamifera*, isolated from a more mature interval than the leiospheres, has a different composition that is more aliphatic and carbon–oxygen abundant, suggesting that biological differences underpin observed spectra.

A representative micro-FTIR spectrum obtained from a single *Shuiyousphaeridium macroreticulatum* from the Ruyang Group is shown in Fig. 3c. The spectrum shows absorptions centered at: a strong broad absorption at 3362 cm^{-1} assigned to alcoholic OH, phenolic OH, and/or carboxylic OH; weak to medium broad aliphatic absorptions between 2700 and 3000 cm^{-1} with a noticeable shoulder at 2960 cm^{-1} and maxima centered at 2920 and 2850 cm^{-1} assigned to asymmetric stretching vibrations from CH_2 and symmetric stretching vibrations from CH_2 methylene groups, respectively; a slight absorption centered at 1710 cm^{-1} assigned to the vibration of carbonyl C=O; a strong absorption of aromatic C=C centered at 1600 cm^{-1}; medium absorption of deformation bending of terminal methyl CH_3 groups centered at 1345 cm^{-1}; and a weak absorption centered at 760 cm^{-1} assigned to =C–H aromatic out-of-plane vibration. A noticeable shoulder appears at 2960 cm^{-1} (asy C–H str of methyl groups) and the width of the band centered at 2929 cm^{-1} is very broad, which indicates a substantial contribution of branched polymethylenic chains. Strong methyl bands and comparatively weaker methylene bands indicate chain branching. In addition, a noticeable shoulder appears at 2955 cm^{-1} (antisymmetric C–H stretch of methyl groups) and the width of the band centered at 2920 cm^{-1} is very broad, which indicates a substantial contribution of branched polymethylenic chains.

In general, micro-FTIR spectra obtained from the Mesoproterozoic acritarchs document a biopolymer with a macromolecular structure of aromatic rings bridged by short branched aliphatic chains. Differences among taxa occur in the relative abundance of aliphatic carbon, degree of branching, and oxygenated functionalities.

3.3. Aliphatic chain length and branching determined by the CH_2/CH_3 ratio

The aliphatic C–H_x stretching vibrational bands in the infrared spectra can be used to assess the chain length and degree of branching of aliphatic side groups within the organic matter of the acritarch cyst wall. If CH_2/CH_3 increases, the aliphatic chains are becoming longer or less branched. Conversely, if the aliphatic chains are short or more branched, the CH_2/CH_3 ratio will be low. An example of the expanded aliphatic C–H_x stretching vibration regions in the curve-fitted spectra of *Tanarium conoideum* and *Leiosphaeridia* sp. is shown in Fig. 4. Five Gaussian/Lorentzian bands can be fitted in the aliphatic C–H_x stretching region (3000–2700 cm^{-1}). These bands are assigned to the following aliphatic structures: 2955 cm^{-1} attributed to antisymmetric CH_3 stretch, 2920 cm^{-1} attributed to antisymmetric CH_2 stretch, 2890 cm^{-1} attributed to CH stretch, 2870 cm^{-1} attributed to symmetric CH_3 stretch, and 2850 cm^{-1} attributed to symmetric CH_2 stretch. Table 3 lists CH_2/CH_3 obtained from curve-fitting of the expanded aliphatic C–H_x stretching vibration of the FTIR spectra acquired from the Neoproterozoic and Mesoproterozoic acritarchs.

It is clear from Table 3 that the organic matter in the *Tanarium conoideum* cyst wall has the highest CH_2/CH_3 ratio (11.10), followed by *Leiosphaeridia*

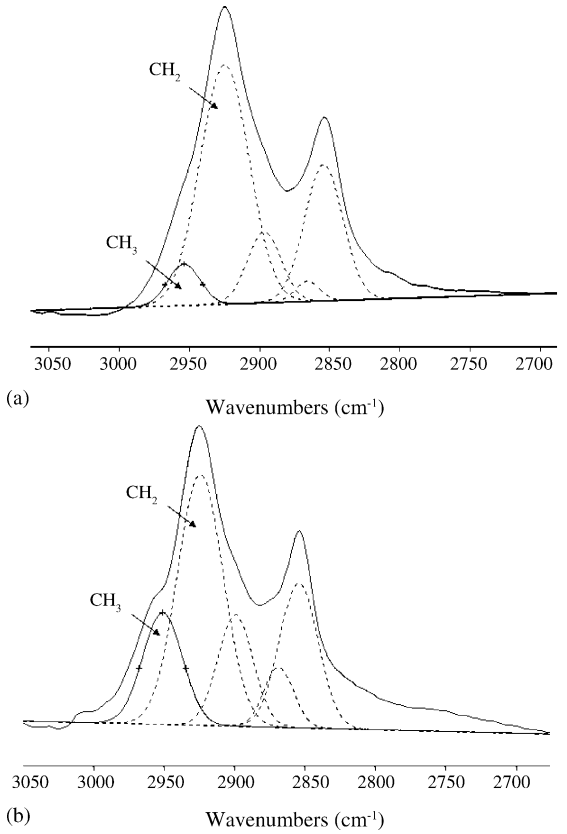

Fig. 4. An example of the expanded aliphatic C–H_x stretching vibration regions (3000–2700 cm^{-1}) and the curve-fitted spectra of acquired from the Neoproterozoic acritarchs (a) *Tanarium conoideum* and (b) *Leiosphaeridia* sp.

sp. (2.47) and *Satka squamifera* (2.40). In contrast CH_2/CH_3 values are ≤2.0 for the other acritarch samples. These results suggest that the acritarch *Tanarium conoideum* contains a biopolymer that consists of aliphatic structures that are long and unbranched. By comparison the other acritarch samples have a CH_2/CH_3 ratio <3.0, signifying a biopolymer containing shorter and more branched aliphatic structures.

Table 3
A list of the CH_2/CH_3 ratios obtained by curve-fitting of the expanded aliphatic C–H_x stretching vibration region of the FTIR spectra acquired from the Neoproterozoic and Mesoproterozoic acritarchs

Acritarch	CH_2/CH_3 ratio
Tanarium conoideum	11.10
Leiosphaeridia sp.	2.47
Leiosphaeridia tenuissima	1.88
Leiosphaeridia jacutica	1.78
Leiosphaeridia crassa	1.99
Shuiyousphaeridium macroreticulatum	2.01
Satka squamifera	2.40

Lin and Ritz (1993) demonstrated the effect of chain length on the infrared CH_2/CH_3 intensity ratios by using a series of known *n*-alkanes. They found a correlation of carbon numbers of *n*-alkanes versus the corresponding CH_2/CH_3 ratios. Using the *n*-alkanes as an oversimplified model (Lin and Ritz, 1993) for the aliphatic structures contained in the organic matter of the acritarch cyst walls, a CH_2/CH_3 value of 11 for *Tanarium conoideum* would correspond to an *n*-alkane chain length of 24 carbons. CH_2/CH_3 values of 2.4 obtained from FTIR analysis of *Leiosphaeridia* sp. and *Satka squamifera* would correspond to a *n*-alkane chain length of 12 carbons, while a CH_2/CH_3 ratio <2 would correspond to a *n*-alkane chain length of eight carbons. We caution, however, that these estimates of average chain length are based on a greatly simplified *n*-alkane model. We will concentrate further work on more complicated model compounds (for example, alkyl benzenes, long-chain fatty acids, and alkyl-substituted cycloalkanes).

3.4. Comparison of functional groups

The functional group frequencies may be viewed quantitatively as well as qualitatively. A given absorption band assigned to a functional group increases proportionately with the number of times that the functional group occurs within the molecule. Aliphatic C–H_x absorption (2920 and 2850 cm^{-1}) and aromatic C=C absorption (1600 cm^{-1}) and their peak intensities were used quantitatively to assess the aromaticity of different acritarch samples. In addition, carbonyl C=O absorption (1710 cm^{-1}) and aromatic C=C absorption (1600 cm^{-1}) and their peak intensities were used quantitatively to assess the abundance of carbon–oxygen functional groups in relation to different acritarch samples. Fig. 5 shows a plot of these ratios obtained from the FTIR spectra of the acritarchs investigated.

Fig. 5 clearly shows that the cell wall of *Tanarium conoideum* is comprised of an aliphatic macromolecular structure that is different from the other acritarch compositions. This result is in agreement with the structural data obtained from deconvolution of the C–H_x stretching region. *Leiosphaeridia* sp. from

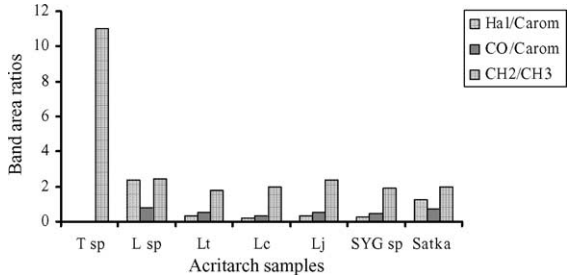

Fig. 5. Plot of peak intensity ratios determined from FTIR spectra of aliphatic C–H (2930–2850 cm^{-1})/aromatic C=C (1600 cm^{-1}) (H_{al}/C_{ar}), carbonyl CO groups (1710 cm^{-1})/aromatic carbon (1600 cm^{-1}) content of the acritarchs (CO/C_{ar}), and the methylene (CH_2)/methyl (CH_3).

the Tanana Formation shows a different biopolymer composition which still consists of linear long chain aliphatic hydrocarbons but has a degree of branching, aliphatic ether bonds, and some olefinic hydrocarbon. *Leiosphaeridia crassa*, *L. jacutica*, *L. tenuissima*, and *Shuiyousphaeridium macroreticulatum* from the Mesoproterozoic Roper and Ruyang groups have similar biopolymer compositions, predominantly aromatic with a low content of highly branched aliphatic chains. The biopolymer composition of *Satka squamifera* biopolymer is notably different, however, in that it contains a greater amount of aliphatic hydrocarbon and carboxyl groups, and the degree of branching is less than the other biopolymer compositions of Roper Group acritarchs.

3.5. Laser micro-Raman spectroscopy

Raman spectra of carbonaceous materials can be divided into two spectral components: the first-order and the second-order spectrum (Vidano and Fischbach, 1978; Nemanich and Solin, 1979). The band assignments will be briefly discussed below for the first-order region; more extensive reviews of various interpretations for the Raman spectra of carbonaceous materials, refer to Dresselhaus and Dresselhaus (1982) and Ferrari and Robertson (2000). The samples analysed in this study do not show spectral features in the second-order region and therefore this region will not be discussed.

The first-order Raman spectrum of hexagonal graphite consists of a single, strong band at 1582 cm^{-1}; this is designated the G band due to the vibrational mode of E_{2g2} symmetry (assigned to in-plane stretching motion of pairs of carbon sp^2 atoms). In addition to this strong band there is a weak band at 42 cm^{-1} due to the E_{2g1} vibrational mode, which is not resolvable from Rayleigh scattering. For disordered sp^2 carbons, additional bands appear at 1150, ~1350, ~1500, and 1620 cm^{-1}. The band at 1150 cm^{-1} occurs in very disordered carbonaceous material, however the assignment is poorly understood. The band at ~1350 cm^{-1} is designated the D band and the origin of this band is poorly understood however; it has been assigned to a breathing mode of A_{1g} symmetry. This mode is forbidden in perfect graphite and only becomes active in the presence of disorder (for example, Ferrari and Robertson, 2000). A broad band around 1500–1550 cm^{-1} has been noticed in several carbon-based materials and was associated with amorphous sp^2 bonded forms of carbon (Nikiel and Jagodzinski, 1993) and is assigned to an amorphous carbon phase. More precisely, it has been suggested that the amorphous carbons can be attributed to interstitial defects (Rouzaud et al., 1983). The band at ~1620 cm^{-1} occurs as a shoulder on the G band and is designated as the D′. The assignment of this band has been attributed to C–C bonds, particularly disrupted bonds at the edges of crystallites (Vidano and Fischbach, 1978; Escribano et al., 2001). This shoulder becomes further developed in more disordered carbonaceous materials, which results in an apparent band broadening and up-shifting of the G band.

The micro-Raman spectra obtained from *Tanarium conoideum* and *Leiosphaeridia* sp. from the Tanana Formation are similar; thus, for brevity, only a representative micro-Raman spectrum obtained from a single *Leiosphaeridia* sp. is shown in Fig. 6a. The carbon first-order spectrum shows a sloping baseline due to fluorescence produced by hydrogen-rich saturated aliphatic hydrocarbons. This result is in agreement with the micro-FTIR spectroscopic data, which indicate a biopolymer consisting of long-chain linear aliphatic molecules.

Fig. 6b–d show spectra with two broad bands at 1605 and 1355 cm^{-1} that are assigned to the G (combination of G and D′ bands producing an apparent band broadening and up-shifting of the G band) and D bands, respectively. The carbon first-order spectra acquired from these acritarchs indicate very weak structural organization and are typical spectra obtained from disordered sp^2 carbons composed of a structurally disordered polynuclear aromatic (PNA) networks.

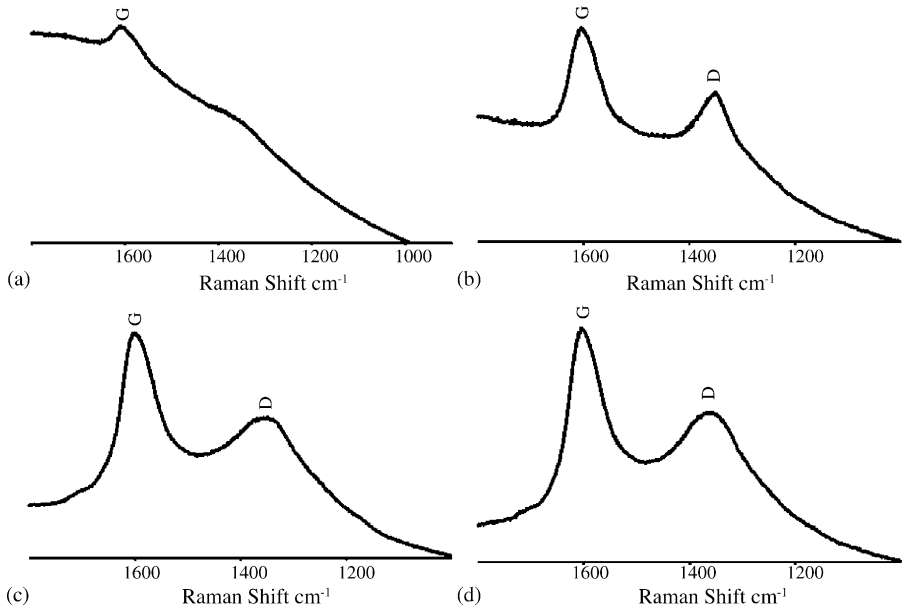

Fig. 6. Representative carbon first-order Raman spectra of the Neoproterozoic acritarch (a) *Leiosphaeridia* sp., and the Mesoproterozoic acritarchs; (b) *Satka squamifera*; (c) *Leiosphaeridia jacutica*; and (d) *Shuiyousphaeridium macroreticulatum*.

Fig. 5b shows a representative carbon first-order spectrum of *Satka squamifera* from the Roper Group. This spectrum shows a moderate sloping base line (in agreement with the FTIR spectra showing more aliphatic carbon in this taxon relative to other Mesoproterozoic taxa); however, two bands can be discerned. Raman spectra collected from *Leiosphaeridia jacutica*, *L. crassa*, *L. tenuissima*, from the Roper Group and the *Shuiyousphaeridium macroreticulatum* from the Ruyang Group show similar line-shapes (Fig. 6c and d). The G band is centered around 1600–1605 cm^{-1} and the D band is centered around 1345–1355 cm^{-1}. The results obtained by Raman spectroscopy are in agreement with the micro-FTIR spectroscopic results, revealing that the acritarch biopolymer consists predominantly of aromatic hydrocarbon bridged by short branched aliphatic chains.

4. Discussion

Our research is centered on evaluating the biological affinities of Proterozoic microfossils. In some cases, morphology provides a reliable guide to systematic interpretation (for example, Butterfield, 2004; Porter et al., 2003), but for many microfossils, morphology alone does not allow phylogenetic placement. Recent work on selected Proterozoic acritarchs (Javaux et al., 2003, 2004a) shows that SEM and especially TEM images of wall ultrastructure can provide further insights into biological relationships. Such research is complemented by micro-FTIR spectroscopy of individual acritarchs, allowing the identification of potentially diagnostic biopolymers (Versteegh and Blokker, 2004), such as the algaenan identified in *Tanarium conoideum*.

Comparative biology can aid in interpreting Proterozoic microfossils by giving the range of modern possibilities for morphology and organic chemical composition of microorganisms. Insoluble non-hydrolysable (INH) biopolymers have been noted in both marine and fresh microalgae, particularly in Chlorophyceae and Eustigmatophyceae (Derenne et al., 1992; Gelin et al., 1999; Versteegh and Blokker, 2004, and references therein). These biomacromolecules, termed algaenans (Tegelaar et al., 1989), are part of the vegetative cell walls and consist of highly aliphatic biopolymers that can be preserved on geological timescales. Algaenans play a major role in kerogen formation via a selective preservation pathway

and can be preserved as ultralaminae (Hatcher et al., 1983; Largeau et al., 1986; Goth et al., 1988; Tegelaar et al., 1989). The wall of the fossil prasinophyte *Tasmanites* may also contain algaenan (see discussion in Versteegh and Blokker, 2004).

In contrast, few studies have been performed on the chemistry of vegetative cell or resting cyst walls from other microorganisms. Prokaryotic biopolymers called cyanobacteran or bacteran have been shown to be artifacts of the isolation procedure (Allard et al., 1997). On the basis of distinct physical properties, biopolymer in dinoflagellate resting cyst walls was given the name dinosporin (to distinguish it from sporopollenin; Sarjeant, 1986). Recently, studies by Kokinos (1994) and Kokinos et al. (1998) of the cysts of the marine dinoflagellate *Lingulodinium polyedrum* revealed it to be made up of a highly resistant aromatic macromolecular substance different from algaenans. More recently, studies of the cyst wall of certain acritarchs from Australian Ediacaran palynofloras suggested that these fossils also contain dinosporin (Arouri et al., 2000), providing chemical evidence of a link between Neoproterozoic acritarchs and dinoflagellates. However, caution must be applied to this interpretation due to the nature of the reported vibrational spectroscopic data. Distinct FTIR signals detected in our study of *Tanarium conoideum* and *Leiosphaeridia* sp. acritarchs contrast with the essentially featureless FTIR spectra recorded for the same samples shown by Arouri et al. (2000). These authors attribute the featureless nature of their IR spectra to the graphitic nature of the acritarch samples. However, the IR spectrum of graphite does not resemble that acquired from their acritarch samples, nor do their Raman spectra resemble spectra obtained from graphite or graphitic-like carbon or well ordered carbon. Our results are, therefore, in disagreement with Arouri et al. (2000), which has a number of implications. The prominent methylene group bands in *Tanarium conoideum* observed by micro-FTIR spectroscopy indicate the highly aliphatic nature of these organisms. This composition is typically obtained from the highly aliphatic biomacromolecule "algaenan" isolated from many species of extant Chlorophycae and Eustigmatophycea microalgae. The acritarch *Leiosphaeridia* sp. from the Tanana Formation may comprise a new class of biopolymer containing significant aliphatic, branched aliphatic and saturated/olefinic carbon molecular constituents, which is different from algaenan, lignin, sporopollenin, or dinosporin macromolecules.

Micro-FTIR analysis of the Mesoproterozoic Roper Group and Ruyang Group acritarchs indicates a biopolymer that is more aromatic in character. Since these acritarchs are of a low thermal maturity (oil window), it is possible that the aromatic character of the acritarch biopolymer does not result from thermal alteration, but rather reflects an indigenous biopolymer containing highly unsaturated material located in structures that are easily transformed into polyaromatic units by low thermal alteration. The FTIR spectra of *Satka squamifera* show a greater component of aliphatic and carbon–oxygen functionality, which would not be expected for a more thermally mature sample. However, a relative opacity may correspond to relative thickness of the microfossil wall, but in other cases the material making up the wall is darker or lighter whatever its thickness and therefore, microfossil colour may not be solely a product of thermal maturity; and may be of some histological, and, thereby, taxonomic significance (Butterfield et al., 1994). Therefore, variations among taxa could, in principle reflect influences of both preservation and phylogeny. In this regard, conclusions presented here should be tested against future studies on same taxa recovered from rocks that have undergone different burial histories.

There have been few reports of highly aromatic biomacromolecules, with the exception of dinoflagellate resting cysts (Kokinos et al., 1998) and *Chlorella marina* (Derenne et al., 1996). However, the aromatic biopolymers described by Derenne et al. (1996) may be due to artifacts created during the isolation procedure (Allard et al., 1997, 1998). Interestingly, recent studies on low thermal maturity Proterozoic kerogens (Brocks et al., 2003) have shown the kerogen to be more similar to modern Type III kerogens (aromatic lignin derived) than to aliphatic-rich Type I (prokaryotic or algal), although Proterozoic organic matter has an exclusively microbial source. Many Mesoproterozoic sedimentary rocks with a mild thermal history contain kerogen that is predominantly aromatic, possibly indicating that Mesoproterozoic organisms might have produced predominantly aromatic insoluble nonhydrolysable (INH) biopolymers. One possibility is that the inferred Mesoproterozoic biopolymers have as yet uncharacterized counterparts in living protists. To date, little work has been done to elucidate biopolymer

compositions of micro-eukaryotes such as euglenids, kinetoplastids, heterokonts, ciliates, red algae, and fungi, indicating a clear need for expanded microchemical and ultrastructural research on living microorganisms.

The three species of leiopheres from the Roper Group show distinct multilayered wall ultrastructures (Javaux et al., 2004a), but similar chemical composition, underscoring the importance of combined morphological, ultrastructural, and microchemical analyses. Conversely, acritarchs with simple morphologies (leiosphaerids), and with very complex ornamentations, wall structure and ultrastructure (*Shuiyousphaeridium macroreticulatum*), have a similar biopolymer composition. The morphology and chemical composition of *Shuiyousphaeridium macroreticulatum* are compatible with a dinoflagellate affinity but could also occur in other microorganisms (Javaux and Marshall, submitted). *Shuiyousphaeridium macroreticulatum* does not show evidence of a trilaminar structure (TLS) in its wall (Javaux et al., 2004a), nor the presence of the aliphatic biopolymer algaenan (this paper); two characteristics of several extant chlorococcalean and eustigmatophycean green algae. However, not all green algae show these features, so their absence in *Shuiyousphaeridium macroreticulatum* does not preclude a green algal affinity for this taxon. Butterfield (2005) suggested a possible fungal affinity for *Shuiyousphaeridium macroreticulatum* based on general morphological similarities with fungal ascocarp (although underlining that this is certainly not established), or at least a multicellular organism not necessarily photoautotrophic. Combined analysis of the fine structure with SEM and TEM show that this acanthomorph acritarch has a reticulate wall of imbricated, beveled polygonal plates (Javaux et al., 2004a), and not of thickened, polygonal cells as might be suggested on the base of light microscopy alone (Butterfield, 2005). This species also shows medial split excystment structures, suggesting a cyst-like morphology, but whether it was a metabolically inert stage of a unicellular or multicellular organism, or whether it had a phototrophic or heterotrophic metabolism, is unknown (Butterfield, 2005; Javaux and Marshall, submitted). On the other hand, *Satka squamifera* displays a morphology (a pack of cells in an envelope) that could be prokaryotic or eukaryotic, and has a slightly different biopolymer composition, as mentioned above. None of the early Mesoproterozoic acritarch walls studied here are composed of algaenan. In summary, then, the biological affinities of Mesoproterozoic acritarchs analyzed to date remain unknown. They could represent stem eukaryotes or extinct crown group clades that produced biopolymers distinct from those of extant groups, or they might belong to extant taxa that synthesize as yet uncharacterized biopolymers.

Our data demonstrate that Raman spectroscopy alone cannot establish the biological affinities of acritarchs; it can provide complementary information on molecular structure when combined with FTIR spectroscopy. The major limitation of Raman spectroscopy in this study resides in only showing the spectral features indicative of disordered sp^2 hybridised carbon bonded to carbon. Typical Raman spectra of ancient kerogens or even of much younger coals (for example, Beny-Bassez and Rouzaud, 1985; Jehlicka et al., 1997; Spotl et al., 1998; Keleman and Fang, 2001) show only sp^2 hybridised carbon bonded to carbon that have undergone degradation in which functional groups are not preserved. However, in more recent biological samples, Raman spectra, acquired at another laser excitation line (1064 nm), show the presence of C=O, C−H, and C−N bonds and pigments, such as β-carotene (Wynn-Williams et al., 2002 and references therein), which can be useful in establishing biological affinity.

5. Conclusions

The Neoproterozoic acritarch *Tanarium conoideum* contains a biopolymer consisting of long chained polymethylenic material which is consistent with algaenan isolated from extant chlorophyte and eustigmatophyte microalgae. On the other hand, the Neoproterozoic acritarch *Leiosphaeridia* sp. may contain a new class of biopolymer containing significant aliphatic, branched aliphatic and saturated/olefinic molecular constituents, different from those of algaenan, lignin, sporopollenin, or dinosporin.

Biopolymer in the walls of Mesoproterozoic acritarchs investigated here consists predominantly of aromatic carbon, with some methylene chains, terminal methyl groups, and carbon-oxygenated functional groups. It is possible that the aromatic character of the acritarch biopolymer does not simply result from

high thermal alteration, but rather reflects an indigenous polyaromatic macromolecule. This is suggested by the more aliphatic composition of the more thermally mature *Satka squamifera* relative to the Mesoproterozoic leiospheres, characterized by a more aromatic biopolymer.

Raman spectroscopy does not provide useful information about the biopolymer composition of Proterozoic acritarchs but rather elucidates the structure and thermal alteration of constituent carbonaceous material. This should be borne in mind when applying micro-Raman spectroscopy to Archean and Proterozoic microfossils.

More research is needed to characterize the chemical and morphological signatures of the full range of recent prokaryotes and protists that produce fossilizable cells. Indeed, a great limitation in detecting the biological affinities of microfossils is our currently limited knowledge of the morphology and chemical composition of decay-resistant cellular structures produced by various living microorganisms. Our ongoing research includes the determination and characterization of resistant biopolymers in a range of living prokaryotes, protists and fungi by combined microscopy and micro-FTIR spectroscopy.

Acknowledgments

We thank Kath Grey for providing Observatory Hill samples and Shuhai Xiao for the Ruyang Group samples. The authors wish to thank one anonymous reviewer, co-Editor Dr. Kenneth Eriksson and Dr. Nick Butterfield for constructive reviews, which have improved the text. Support came from Exobiology Grant NAG5-3645 and the NASA Astrobiology Institute, the Australian Research Council and Macquarie University, and the Belgian Science Federal Policy Office.

References

Allard, B., Templier, J., Largeau, C., 1997. Artifactual origin of mycobacterial bacteran: formation of melanoidin-like artifactual macromolecular material during the usual isolation process. Org. Geochem. 26, 691–703.

Allard, B., Templier, J., Largeau, C., 1998. An improved method for the isolation of artifact-free algaenans from microalgae. Org. Geochem. 28, 543–548.

Anbar, A.D., Knoll, A.H., 2002. Proterozoic ocean chemistry and evolution: a bioinorganic bridge? Science 297, 1137–1142.

Arouri, K., Greenwood, P.F., Walter, M.R., 1999. A possible chlorophycean affinity of some Neoproterozoic acritarchs. Org. Geochem. 30, 1323–1337.

Arouri, K., Greenwood, P.F., Walter, M.R., 2000. Biological affinities of Neoproterozoic acritarchs from Australia: microscopic and chemical chacacterisation. Org. Geochem. 31, 75–89.

Batten, D.J., 1996. Palynofacies and petroleum potential. In: Jansonius, J., McGregor, D.C. (Eds.), Palynology: Principles and Applications, vol. 3. American Association of Stratigraphic Palynologists Foundation, pp. 1065–1084.

Beny-Bassez, C., Rouzaud, J.N., 1985. Characterisation of carbonaceous materials by correlated electron and optical microscopy and Raman microspectroscopy. Scanning Electron Microsc. 1, 119–132.

Brocks, J.J., Love, G.D., Snape, C.E., Logan, G.A., Summons, R.E., Buick, R., 2003. Release of bound aromatic hydrocarbons from late Archean and Mesoproterozoic kerogens via hydropyrolysis. Geochim. Cosmochim. Acta 67, 1521–1530.

Brooks, J., Shaw, G., 1971. Recent developments in the chemistry, biochemistry, geochemistry and post-tetrad ontogeny of sporopollenins derived from pollen and spore exines. In: Heslop-Harrison, J. (Ed.), Pollen Development and Physiology. Appleton-Century-Crofts, New York, pp. 99–194.

Butterfield, N.J., Knoll, A.H., Swett, K., 1994. Paleobiology of the Neoproterozoic Svanbergfjellet Formation, Spitsbergen. Fossils Strata 34, 1–84.

Butterfield, N.J., 2000. *Bangiomorpha pubescens* n. gen., n. sp.: implications for the evolution of sex, multicellularity and the Mesoproterozoic–Neoproterozoic radiation of eukaryotes. Paleobiology 26, 386–404.

Butterfield, N.J., 2004. A vaucheriacean alga from the middle Neoproterozoic of Spitsbergen: implications for the evolution of Proterozoic eukaryotes and the Cambrian explosion. Paleobiology 30, 231–252.

Butterfield, N.J., 2005. Probable Proterozoic Fungi. Paleobiology 31 (1), 165–182.

Colbath, G.K., Grenfell, H.R., 1995. Review of biological affinities of Paleozoic acid-resistant, organic walled eukaryotic algal microfossils (including acritarchs). Rev. Palaeobot.Palynol. 86, 287–314.

Derenne, S., Largeau, C., Berkaloff, C., Rousseau, B., Wilhelm, C., Hatcher, P.G., 1992. Non-hydrolysable macromolecular constituents from outer walls of Chlorella fusca and Nanochlorum eucaryotum. Phytochemistry 31, 1923–1929.

Derenne, S., Largeau, C., Berkaloff, C., 1996. First example of an algaenan yielding an aromatic-rich pyrolysate. Possible geochemical implications on marine kerogen formation. Org. Geochem. 24, 617–627.

Douzery, E.J.P., Snell, E.A., Bapteste, E., Delsuc, F., Philippe, H., 2004. The timing of eukaryotic evolution: does a relaxed molecular clock reconcile proteins and fossils? Proc Natl. Acad. Sci. U.S.A. 101 (43), 15386–15391.

Downie, C., Evitt, W.R., Sarjeant, W.A.S., 1963. Dinoflagellates, hystrichospheres, and the classification of the acritarchs. Stanford University Publications, Geological Sciences, vol. 7, pp. 1–16.

Dresselhaus, M.S., Dresselhaus, G., 1982. In: Cardona, M., Guntherodt (Eds.), Light Scattering in Solids III. Springer, Berlin, p. 187.

Escribano, R., Sloan, J.J., Siddique, N., Sze, N., Dudev, T., 2001. Raman spectroscopy of carbon-containing particles. Vib. Spectrosc. 26, 179–186.

Ferrari, A.C., Robertson, J., 2000. Interpretation of Raman spectra of disordered and amorphous carbon. Phys. Rev. B: Condens. Matter Mater. Phys. 61, 14095–14107.

Gelin, F., Volkman, J.K., Largeau, C., Derenne, S., Sinninghe Damste, J.S., De Leeuw, J.W., 1999. Distribution of aliphatic, nonhydrolyzable biopolymers in marine microalgae. Org. Geochem. 30, 147–159.

Goth, K., de Leeuw, J.M., Puttmann, W., Tegelaar, E.W., 1988. Origin of Messel oil shale kerogen. Nature 336, 759–761.

Grey, K., 1998. Ediacarian acritarchs of Australia. Ph.D. thesis, Macquarie University.

Hatcher, P.G., Spiker, E.C., Szeverenyi, N.M., Maciel, G.E., 1983. Selective preservation and origin of petroleum forming aquatic kerogen. Nature 305, 498–501.

Javaux, E.J., Knoll, A.H., Walter, M.R., 2001. Morphological and ecological complexity in early eukaryotic ecosystems. Nature 412, 66–69.

Javaux, E.J., Knoll, A.H., Walter, M.R., 2003. Recognizing and interpreting the fossils of Early Eukaryotes. Origins Life Evol. Biosphere 33, 75–94.

Javaux, E.J., Knoll, A.H., Walter, M.R., 2004a. TEM evidence for eukaryotic diversity in mid-Proterozoic oceans. Geobiology 2, 121–132.

Javaux, E.J., Knoll, A.H., Marshall, C.P., Walter, M.R., 2004b. Recognizing early life on Earth and Mars. European Space Agency Special Paper, vol. 545, pp. 127–130.

Javaux, E.J., Marshall, C.P., submitted. A new approach in deciphering early protist paleobiology and evolution: combined microscopy and microchemistry of single acritarchs.

Jehlicka, J., Beny, C., Rouzaud, J-N., 1997. Raman microspectrometry of accumulated non-graphitized solid bitumens. J. Raman Spectrosc. 28, 717–724.

Keleman, S.R., Fang, H.L., 2001. Maturity trends in Raman spectra from kerogen and coal. Energy Fuels 15, 653–658.

Kjellstrom, G., 1968. Remarks on the chemistry and ultrastructure of the cell wall of some Palaeozoic leiospheres. Geol. Foreningens Stockholm Forhandl. 90, 221–228.

Knoll, A.H., 1996. Archaean and Proterozoic palaeontology. In: Jansonius, J., McGregor, D.C. (Eds.), Palynology: Principles and Applications, vol. 1, American Association of Stratigraphic Palynologists Foundation. Publishers Press, Salt Lake City, pp. 51–80, Chapter 4.

Kokinos, J.P., 1994. Studies on the cell wall of dinoflagellate resting cysts: morphological development, ultrastructure, and chemical composition. Ph.D. thesis, Massachusetts Institute of Technology/Woods Hole Oceanographic Institution, Technical Report WHOI-94-10.

Kokinos, J.P., Eglinton, T.I., Goñi, M.A., Boon, J.J., Martoglio, P.A., Anderson, D.M., 1998. Characterization of a highly resistant biomacromolecular material in the cell wall of a marine dinoflagellate resting cyst. Org. Geochem. 28, 265–288.

Largeau, C., Derenne, S., Casadevall, E., Kadouri, A., Sellier, N., 1986. Pyrolysis of immature Torbanites and of the resistant biopolymer (PRB A) isolated from extant alga *Botryococcus braunii*. Mechanism of formation and structure of Torbanite. Org. Geochem. 10, 1023–1032.

Lin, R., Ritz, G.P., 1993. Studying individual macerals using i.r. microspectroscopy, and implications on oil versus gas/condensate proneness and low rank generation. Org. Geochem. 20, 695–706.

Moldowan, J.M., Talyzina, N.M., 1998. Biogeochemical evidences for dinoflagellate ancestors in the Early Cambrian. Science 281, 1168–1170.

Martin, F., 1993. Acritarchs: a review. Biol. Rev. 68, 475–538.

Nemanich, R.J., Solin, S.A., 1979. First- and second-order Raman scattering from finite-size crystals of graphite. Phys. Rev. B 20, 392–401.

Nikiel, L., Jagodzinski, P.W., 1993. Raman spectroscopic characterization of graphites: a re-evaluation of spectra/structure correlation. Carbon 31, 1313–1317.

Painter, P.C., Snyder, R.W., Starsinic, M., Coleman, M.M., Kuehn, D.W., Davis, A., 1985. Concerning the application of FTIR to the study of coal: a critical assessment of band assignments and the application of spectral analysis programs. Appl. Spectrosc. 35, 475–485.

Porter, S.M., Meisterfeld, R., Knoll, A.H., 2003. Vase-shaped microfossils from the Neoproterozoic Chuar Group, Grand Canyon: a classification guided by modern testate amoebae. J. Paleontol. 77, 409–429.

Rouzaud, J.N., Oberlin, A., Beny-Bassez, C., 1983. Carbon film: structure and microtexture (optical and electron microscopy, Raman Spectroscopy). Thin Solid Films 105, 75–96.

Sarjeant, W.A.S., 1986. Review of Evitt, W.R., 1985. Sporopollenin Dinoflagellate Cysts: their morphology and interpretation. Micropaleontology 32, 282–285.

Sarjeant, W.A.S., Stancliffe, R.P.W., 1994. The Micrhystridum and Veryhachium complexes (Acritarcha: Acanthomorphitae and Polygonomorphitae) a taxonomic reconsideration. Micropaleontology 40, 1–77.

Senftle, J.T., Landis, C.R., 1991. Vitrinite reflectance as a tool to assess thermal maturity. In: Merrill, R.K. (Ed.), Source and Migration Processes and Evaluation Techniques; Treatise of Petroleum Geology. American Association of Petroleum Geologists, Tulsa, pp. 119–125.

Solomon, P.R., Carangelo, R.M., 1987. FTIR analysis of coal. Fuel 67, 949–959.

Spotl, C., Houseknecht, D.W., Jaques, R.C., 1998. Kerogen maturation and incipient graphitization of hydrocarbon source rocks in the Arkoma Basin Oklahoma and Arkansas: a combined petrographic and Raman spectrometric study. Org. Geochem. 28, 535–542.

Staplin, F.L., Jansonius, J., Pocock, S.A.J., 1965. Evaluation of some Acritarchous Histrichoshere genera. Neues Jahrb. Geol. Palaontol. 123, 167–201.

Su, H., Hackett, Y.D., Ciniglia, C., Pinto, G., Bhattacharya, D., 2004. A molecular timeline for the origin of photosynthetic eukaryotes. Mol. Biol. Evol. 21 (5), 809–818.

Talyzina, N.M., Moczydlowska, M., 2000. Morphological and ultrastructural studies of some acritarchs from the Lower Cambrian Lukati Formation, Estonia. Rev. Palaeobot. Palynol. 112, 1–21.

Talyzina, N.M., Moldowan, J.M., Johannisson, A., Fago, F.J., 2000. Affinities of Early Cambrian acritarchs studied by using microscopy, fluorescence flow cytometry and biomarkers. Rev. Palaeobot. Palynol. 108, 37–53.

Tappan, H., 1980. The Paleobiology of Plant Protists. Freeman, San Franciso, CA, pp. 148–224.

Tegelaar, E.W., de Leeuw, J.W., Derenne, S., Largeau, C., 1989. A reappraisal of kerogen formation. Geochim. Cosmochim. Acta 53, 3103–3106.

Traverse, A., 1988. Paleopalynology. Unwin Hyman, London, 600 pp.

Van Waveren, I., 1992. Morphology of probable planktonic crustacean eggs from the Holocene of the Banda Sea (Indonesia). In: Head, M.J., Wrenn, JH. (Eds.), Neogene and Quaternary Dinoflagellate Cysts and Acritarchs. American Association of Stratigraphic Palynologists Foundation, Dallas, pp. 89–120.

Versteegh, G.J.M., Blokker, P., 2004. Resistant macromolecules of extant and fossil microalgae. Phycol. Res. 52, 325–339.

Vidano, R., Fischbach, D.B., 1978. New lines in the Raman spectra of carbons and graphite. J. Am. Ceram. Soc. 61, 13–17.

Wall, D., 1958. Evidence from recent plankton regarding the biological affinities of Tasmanites Newton 1875 and Leiosphaeridia Eisenack. Geol. Mag. 4, 353–362.

Wynn-Williams, D.D., Edwards, H.G.M., Newton, E.M., Holder, J.M., 2002. Pigmentation as a survival strategy for ancient and modern photosynthetic microbes under high ultraviolet stress on planetary surfaces. Int. J. Astrobiol. 1, 39–49.

Xiao, S., Knoll, A.H., Zhang, Y., Yin, L., 1997. Neoproterozoic fossils in Mesoproterozoic rocks? Chemostratigraphic resolution of a biostratigraphic conundrum from the North China Platform. Precambrian Res. 84, 197–220.